Hydrol. Earth Syst. Sci. Discuss., 11, 1529–1554, 2014
www.hydrol-earth-syst-sci-discuss.net/11/1529/2014/
doi:10.5194/hessd-11-1529-2014

Hydrology and Earth System Sciences
Discussions
Open Access

Attribution of satellite observed vegetation trends in a hyper-arid region of the Heihe River Basin, Central Asia

Y. Wang[1,2,3], **M. L. Roderick**[3,4,5], **Y. Shen**[1], **and F. Sun**[3,5]

[1]Key Laboratory of Agricultural Water Resources, Hebei Key Laboratory of Agricultural Water-Saving, Center for Agricultural Resources Research, Institute of Genetics and Developmental Biology, Chinese Academy of Sciences, Shijiazhuang 050021, China
[2]University of Chinese Academy of Sciences, Beijing 10049, China
[3]Research School of Biology, The Australian National University, Canberra 0200, Australia
[4]Research School of Earth Science, The Australian National University, Canberra 0200, Australia
[5]Australian Research Council Centre of Excellence for Climate System Science

Received: 8 December 2013 – Accepted: 9 January 2014 – Published: 5 February 2014

Correspondence to: Y. Shen (yjshen@sjziam.ac.cn)

Published by Copernicus Publications on behalf of the European Geosciences Union.

Abstract

Terrestrial vegetation dynamics are closely influenced by both climate change and by direct human activities that modify land use and/or land cover (LULCC). Both can change over time in a monotonic way and it can be difficult to separate the effects of climate change from LULCC on vegetation. Here we attempt to attribute the trend of fractional green vegetation cover to climate change and to human activity in Ejina region, a hyper-arid landlocked region in northwest China. This region is dominated by extensive deserts with relatively small areas of irrigation located along the major water courses as is typical throughout much of Central Asia. Variations of fractional vegetation cover from 2000 to 2012 were determined using Moderate Resolution Imaging Spectroradiometer (MODIS) vegetation index data with 250 m spatial resolution over 16 day intervals. We found that the fractional vegetation cover in this hyper-arid region is very low, but that the mean growing season vegetation cover has increased from 3.4 % in 2000 to 4.5 % in 2012. The largest contribution to the overall greening was due to changes in green vegetation cover of the extensive desert areas with a smaller contribution due to changes in the area of irrigated land. Comprehensive analysis with different precipitation data sources found that the greening of the desert was associated with increases in regional precipitation. We found that the area of land irrigated each year was mostly dependent on the runoff gauged one year earlier. Taken together, water availability both from precipitation in the desert and runoff inflow for the irrigation agricultural lands can explain at least 52 % of the total variance in regional vegetation cover from 2000 to 2010.

1 Introduction

Terrestrial vegetation plays a key role in energy, water and biogeochemical cycles and changes in vegetation can also significantly influence atmospheric processes (Pielke et al., 1998; Gerten et al., 2004). Monitoring of terrestrial vegetation dynamics

HESSD
11, 1529–1554, 2014

therefore underpins efforts to better understand the feedbacks between vegetation and the atmosphere (Bonan et al., 2003; Bounoua et al., 2010; Angelini et al., 2011). In particular, the Normalized Difference Vegetation Index (NDVI) derived from satellite observations of red and near-infrared reflectance has proven useful in assessing vegetation dynamics from regional to global scales (Tucker, 1979; Box et al., 1989; Fensholt et al., 2013).

Greening trends have been detected on global (Myneni et al., 1997; Nemani et al., 2003; Donohue et al., 2013; Fensholt et al., 2013) and regional (Fang et al., 2004; Herrmann et al., 2005; Donohue et al., 2009) scales but attribution of those trends in terms of the underlying biophysical and socio-economic causes remains a difficult task. The central challenge is that vegetation can change for a myriad of reasons including changes in the local climate (e.g., rainfall, radiation, temperature, humidity, etc.), biogeochemistry (e.g., atmospheric CO_2, nutrient deposition, etc.), ecological processes (e.g. long term successional recovery from disturbance, fire dynamics, disease, etc.) and via direct anthropogenic activity (e.g., land use change, irrigation, agriculture, etc.). One approach to handle this complexity is to use regional knowledge to constrain the problem.

In terms of the attribution of regional vegetation trends, Central Asia presents a unique challenge. The region is hyper-arid with annual precipitation in many areas often less than 50 mm with hot summers and cold winters. What is of particular interest throughout Central Asia is the presence of many localised regions of irrigated agriculture that often support relatively large local populations. Those irrigation communities are usually located at oases that receive an annual input of water in the form of runoff from surrounding mountains. Much of the outflow from the mountains is recent precipitation (snow-melt) but a further complication of recent years is that glacier melt has augmented the snow melt and increased inflow of water to many oases throughout Central Asia (Yao et al., 2004; Lioubimtseva and Henebry, 2009; Rahimov, 2009; Unger-Shayesteh et al., 2013). Time series of NDVI satellite imagery generally show greening trends over Central Asia, especially before 2000 (Fang et al., 2004;

HESSD
11, 1529–1554, 2014

Mohammat et al., 2013). However, in terms of overall water resources management it is important to understand whether an overall greening (or browning) trend arose because of an expansion (or contraction) of the area being irrigated. Alternatively, the irrigated area might have remained more or less constant and any large scale greening (or browning) trend in vegetation might be related to subtle yet detectable changes in vegetation cover in the extensive deserts in Central Asia. The management implications are quite different for those two scenarios and require a clear separation of these sources of variation.

In this paper, we investigate satellite observed (MODIS) vegetation trends (NDVI) in a hyper-arid region of the Heihe River Basin located in northwest China. The aim of this study is to test whether it is possible to separate the vegetation trends in a small relatively well studied basin into a component due to greening (browning) of the deserts and a second component due to changes in irrigation. We anticipate that the method might be widely applicable throughout Central Asia.

2 Data and methods

2.1 Study area

We examine part of the landlocked Heihe River Basin in northwest China (40°20′–42°40′ N, 97°30′–101°45′ E). Our study area occupies the downstream (northern) part of the basin (Fig. 1b) and is serviced by the regional centre, Ejina, which currently has a population of around 30 000 (GeoHive, 2010). The hydro-climate of this predominantly desert environment is extreme. As an indication, at Ejina, the mean annual temperature is around 8 °C but day-time excursions in the summer reach 42 °C whilst night-time temperatures drop to −36 °C during winter (Zhang et al., 2011). The mean annual precipitation over the extensive non-mountain regions is typically less than 50 mm (Fig. 1a) while the mean annual pan evaporation is typically around 3500 mm (Jin et al., 2010; Jia et al., 2011; Wang et al., 2013). Agriculture is only

HESSD
11, 1529–1554, 2014

possible via irrigation that is located immediately adjacent to the Heihe River (Fig. 1). The study area (~ 80 000 km^2) is located with the broader Gobi desert and also hosts the second largest area of *Populus euphratica* and *Haloxylon ammondendron* forests in China. The basin is generally considered to be the main eco-barrier in northern China (Fu et al., 2007; Qin et al., 2012).

The Heihe River (Fig. 1b) is the second longest inland river in China and is the sole river flowing through the Ejina region (Guo et al., 2009). This river originates in the Qilian Mountains. After reaching the mountain outlet at the Yingluoxia hydrological gauge station (Fig. 1b), it flows through several oases (Zhangye, Gaotai, Dingxin, Ejina) before terminating at the East and West Juyan Lakes. Zhengyixia station is located downstream of those main oases, where the most water was consumed for agriculture. The discharge at Zhengyixia typically peaks around September each year while the growing season extends from April to October (Fig. 2a). Consequently, the irrigated crops in the northern parts of the basin use irrigation water that was discharged from the mountains some 6 months earlier.

The river discharge from the mountain regions showed increase trend in past decades. Annual discharge observed at Yingluoxia site increased to 15.7×10^8 m^3 in the 1990s from around 14.4×10^8 m^3 in the 1960s (Fig. 2b). However, the discharge observed at Zhengyixia station located at the place after the river flow through the oases decreased from around 10.5×10^8 m^3 in the 1960s to around 7.5×10^8 m^3 in the 1990s. The increasing water withdrawal in the upper and middle reaches since the 1960s was associated with increased irrigation (and associated industrial development and urbanization) that made significant reduction in river flows to the downstream oases and accelerated desertification in the northern parts of the basin (Guo et al., 2009; Jin et al., 2010). This phenomenon resulted in the drying-up of East Juyan Lake in 1992 and the drying-up of West Juyan Lake even earlier (Guo et al., 2009).

To restore the ecosystem of the downstream Heihe basin the Ecological Water Conveyance Project (EWCP) was launched by the Chinese Government. Water use has been regulated (reduced) since around the year 2000 in the middle parts of the

HESSD
11, 1529–1554, 2014

basin thereby delivering more water to the northern parts (Zhang et al., 2011). In the past decade (2000–2009) the average flow at Zhengyixia has increased to levels (about 10.5×10^8 m^3) not seen much since the 1960s (Zhang et al., 2011; Qin et al., 2012). This extra water has restored degradation of the ecological environment in the northern extremities. Since 2000, an increase in native vegetation growth and species diversity has been attributed to increased groundwater recharge from the increased flows making their way into the northern parts of the basin (Jin et al., 2010; Jia et al., 2011).

In summary the basin is a classic source-sink system with water sourced (via snow- and glacier-melt) in the humid mountains in the south that subsequently flows northwards to terminal sinks at the East and West Juyan lakes. With that background we note that many studies have reported trends in vegetation in particular subregions of the basin (Jin et al., 2010; Jia et al., 2011; Wang et al., 2011) but there has yet to be a comprehensive assessment of vegetation trends in the study area. A basin-wide assessment that is useful for hydrologic management requires separation of the overall vegetation trend into a component due to irrigation and a component due to changes in the desert vegetation. That is the aim of the current study.

2.2 MODIS satellite observations

Moderate Resolution Imaging Spectroradiometer (MODIS) Terra Vegetation Indices (MOD13Q1) data were acquired from the National Aeronautics and Space Administration (NASA) Earth Observing System Data and Information System (NASA, 2013) with spatial resolution of 250 m and temporal resolution of 16 days between April 2000 and December 2012. We initially used the Savitzky–Golay filter (Chen et al., 2004) to minimise noise in the NDVI series prior to further processing. Exploratory analysis highlighted anomalously low NDVI values during many of the winter months that coincided with snow/ice cover. To avoid those anomalous values we restricted the time series to cover the seven month growing season (April–October).

HESSD
11, 1529–1554, 2014

2.3 Identifying the irrigated areas

The irrigation regions of interest are restricted to the immediate vicinity of the Heihe River (within the dashed line in Fig. 1c). Within that zone, irrigation is usually supplied by the extraction of groundwater and it is very difficult to distinguish agricultural vegetation from native vegetation that is drawing upon groundwater reserves in the satellite imagery. However, both vegetation types use the same groundwater resources and we make no distinction between them. That enabled us to use a simple threshold approach to identify the vegetation areas of interest because they have much higher green vegetation cover during the April–October growing season. To identify those areas we created a composite image for each year (2000–2012) showing the maximum NDVI recorded during the April–October growing period. By trial and error we found that if the annual maximum NDVI was greater than 0.1, the area could be considered irrigation (including groundwater dependent native vegetation) provided it was within the immediate environment of the Heihe River, i.e., also within the dashed line shown in Fig. 1c. The threshold was used to classify the land cover into two classes, desert and irrigation, for each year of the period 2000–2012.

2.4 Converting NDVI to Fractional Vegetation Cover

Fractional Vegetation Cover (f_V) was computed from NDVI (V) using a simple linear scaling (Carlson and Ripley, 1997):

$$f_V = (V - V_{min})/(V_{max} - V_{min}) \quad (1)$$

where V_{min} and V_{max} represent zero green vegetation cover (i.e., bare soil, $f_V = 0$) and complete foliage cover ($f_V = 1$) respectively. We assume that there are regions of bare soil (e.g., desert) and of complete foliage cover (e.g., irrigated agriculture) in the study area of sufficient size relative to the MODIS spatial resolution (250 m) to define the limits of our scaling. To identify those limits we first composited the annual (April–October) maximum V image into a single maximum V image for the entire 13 yr (2000–

HESSD
11, 1529–1554, 2014

2012) study period. We then conducted a detailed examination of the desert regions and identified an NDVI threshold of 0.05 that was equated to bare ground ($f_V = 0$). To identify the upper limit we investigated small regions of agricultural crops in the maximum composite and identified an NDVI threshold of 0.65 that was equated to full cover ($f_V = 1$). Those thresholds were used (in Eq. 1) to re-scale the NDVI data into foliage cover with values outside the range set to the respective limits.

2.5 Attribution of vegetation changes

With the region split into two land cover types, the regional fractional vegetation cover (f_V) is determined by fractional vegetation coverage of the irrigated (f_I) and non-irrigated (f_D) areas and the respective areas (A_I,A_D) for each year,

$$f_V = \frac{A_I \cdot f_I + A_D \cdot f_D}{A_I + A_D} \tag{2}$$

Defining the area fractions $A_I^* \left(= \frac{A_I}{A_I + A_D}\right)$ and $A_D^* \left(= \frac{A_D}{A_I + A_D}\right)$ with $A_I^* + A_D^* = 1$, we can rewrite Eq. (2) as,

$$f_V = A_I^* \cdot f_I + A_D^* \cdot f_D \tag{3}$$

The full differential $\mathrm{d}f_V$ is:

$$\begin{aligned} \mathrm{d}f_V &= \frac{\partial f_V}{\partial f_I}\mathrm{d}f_I + \frac{\partial f_V}{\partial A_I^*}\mathrm{d}A_I^* + \frac{\partial f_V}{\partial f_D}\mathrm{d}f_D + \frac{\partial f_V}{\partial A_D^*}\mathrm{d}A_D^* \\ &= A_I^*\,\mathrm{d}f_I + f_I\,\mathrm{d}A_I^* + A_D^*\,\mathrm{d}f_D + f_D\,\mathrm{d}A_D^* \end{aligned} \tag{4}$$

The relative change in f_V is given by,

$$\frac{\mathrm{d}f_V}{f_V} = \frac{A_I^* f_I}{f_V}\frac{\mathrm{d}f_I}{f_I} + \frac{f_I}{f_V}\mathrm{d}A_I^* + \frac{A_D^* f_D}{f_V}\frac{\mathrm{d}f_D}{f_D} + \frac{f_D}{f_V}\mathrm{d}A_D^* = X_{fI} + X_{AI} + X_{fD} + X_{AD} \tag{5}$$

where the various X terms denote the total change in f_V due to changes in the greenness (X_{fI}, X_{fD}) and fractional area (X_{AI}, X_{AD}).

HESSD
11, 1529–1554, 2014

2.6 Estimates of water availability

The vegetation trends are ultimately compared to estimates of trends in water availability over the desert and in the irrigation area. We use the monthly discharge gauged at Zhengyixia (Fig. 1b) as a measure of the inflow available for irrigation in Ejina. Over the desert parts of the region, precipitation represents the only input of water. To estimate water availability via precipitation we use three gridded databases (0.5° ×0.5°, monthly, 2000–2010) from the Global Precipitation Climatology Centre (GPCC) (Schneider et al., 2008), Climatic Research Unit (CRU) TS 3.10 (Harris et al., 2013) and the Climate Prediction Center (CPC) (Chen et al., 2002). We also average the data from two local meteorological sites (Ejina, Dingxin; see Fig. 1b) as a further check on the gridded databases. Initial analysis showed that precipitation (P) was generally a little higher in the CRU database (but with similar inter-annual variability) while the other two remaining databases gave almost identical results (Fig. 3). We were most familiar with the GPCC database following previous work (Sun et al., 2012) and subsequently adopted the GPCC database as the precipitation record for the study area. Note that final interpretations and our conclusions are not sensitive to the choice of precipitation database and we also present the complete analysis using the other spatial databases (CRU, Sites, and CPC) in the supporting material.

3 Results

3.1 Vegetation trends

The fractional vegetation cover f_V in this hyper-arid region is very low, with mean growing season f_V of about 3–4 %. The oasis systems are clearly distinguished by the much higher vegetation cover (Fig. 4a). Over the 13 yr period (2000–2012) the mean growing season foliage cover (f_V) showed a more or less steady increase starting at about 3.2 % in 2000 and rising to around to 4.5 % in 2012 (Fig. 4b). Fractional

HESSD
11, 1529–1554, 2014

vegetation cover in both the desert and irrigated regions also increased and more or less tracked the increase in f_V.

The mean growing season foliage cover in the extensive desert regions (f_D) more or less tracked the changes in the regional total (f_V). The area classified as irrigated only occupies around 3 % of total study area with a relatively high growing season average vegetation cover f_I of around 17 %. Over the 2000–2012 period, the fractional irrigation area (A_I^*) showed a steady increase (from 3 to 4 %) and the mean growing season foliage cover (f_I) also increased from around 16–18 %.

3.2 Trend attribution

3.2.1 Sensitivity

After substituting the relevant numerical values ($f_V = 0.039$, $f_I = 0.174$, $A_I^* = 0.033$, $f_D = 0.035$, $A_D^* = 0.967$) derived from the mean growing season (2000–2012) into Eq. (5), the relative change in f_V is,

$$\frac{df_V}{f_V} = 0.15\frac{df_I}{f_I} + 4.45dA_I^* + 0.85\frac{df_D}{f_D} + 0.88dA_D^* \quad (6)$$

The coefficients in Eq. (6) denote the different sensitivity to change in the overall regional vegetation cover. The most sensitive factor is relative variations in the fractional irrigated area (A_I^*). Note that regional vegetation cover is also a factor of around six (= 0.85/0.15) more sensitive to variations in greenness over the desert than over the irrigated regions because the desert land cover type dominates the total area.

3.2.2 Trend attribution

From 2000 to 2012, the regional f_V increased by ~ 25 %. In terms of the underlying components, the causes of those changes varied from year to year (Fig. 5) but the largest contribution was generally due to changes in f_D (see X_{fD} in Fig. 5) with a smaller

HESSD
11, 1529–1554, 2014

contribution due to changes in A_I^* (X_{AI} in Fig. 5). Variations in the remaining terms (X_{fI}, X_{AD}) had little impact on trends in the overall regional vegetation cover.

3.3 Predicting regional vegetation cover based on water availability

The earlier results (Sect. 3.2.2) show that the regional vegetation cover trend mainly depends on fractional vegetation cover over the extensive desert regions and the area of the irrigated lands. With that result, we approximate Eq. (5) as,

$$\frac{df_V}{f_V} \sim \frac{f_I}{f_V} dA_I^* + \frac{A_D^*}{f_V} df_D \tag{7}$$

In this region the area of land irrigated each year is dependent on the inflow at an earlier time while greenness in the desert areas is dependent on precipitation. To test that we use the 12 month precipitation to the end of the growing season (previous November–October) to estimate the growing season desert vegetation cover. The results when using GPCC precipitation show a positive relationship ($p < 0.05$, Fig. 6) and imply that the desert vegetation cover increases by 0.017 % for each additional mm of P. (The analysis based on other precipitation databases (CRU, Sites, and CPC) is included in the supporting materials (Fig. S1 and Table S1)).

We sought a similar predictive relation between the total runoff in the previous calendar year at Zhengyixia and the fractional irrigated area (A_I^*) (Fig. 7). The results (Fig. 7) reveal a strong positive relationship ($p = 0.002$) where an increase in inflow at Zhengyixia of 1×10^8 m^3 will increase the fractional area of irrigation by around 0.1 %.

The results allow us to modify the earlier expression by replacing dA_I^* with $\alpha\, dR$ (Fig. 5) and df_D with $\beta\, dP$ respectively,

$$\frac{df_V}{f_V} \sim \frac{f_I}{f_V} \alpha\, dR + \frac{A_D^*}{f_V} \beta\, dP \tag{8}$$

HESSD
11, 1529–1554, 2014

Expressing that in a relative form we have,

$$\frac{\mathrm{d}f_V}{f_V} \sim \frac{f_I}{f_V}\alpha R\frac{\mathrm{d}R}{R} + \frac{A_D^*}{f_V}\beta P\frac{d\mathrm{P}}{P}$$

Taking the long term mean annual values ($f_I = 0.17$, $f_V = 0.038$, $R = 9.67$, $P = 47.54$, $A_D^* = 0.97$) and the empirical coefficients ($\alpha = 0.0011$, Fig. 7; $\beta = 0.00017$, Fig. 6) we have,

$$\frac{\mathrm{d}f_V}{f_V} \sim 0.05\frac{\mathrm{d}R}{R} + 0.21\frac{\mathrm{d}P}{P} = X_R + X_P \quad (9)$$

The empirically based equation predicts that a 1 % variation in runoff would leads to a 0.05 % variation in f_V whilst a 1 % variation in precipitation would increase f_V by 0.21 %. Finally we use the runoff and precipitation data to estimate the relative changes in regional vegetation cover. The overall result shows that the model developed here accounts for at least 52 % of the total variance in regional vegetation cover (Fig. 8).

4 Discussions

In this study, we focus on an oasis-desert system where agricultural crops and groundwater-fed native vegetation that occupy some 4 % of the entire region are concentrated along the Heihe River. We were able to identify the crops and green native vegetation along the river from the elevated NDVI signal during the April–October growing season. Each year we identified those regions but we were unable to separate the crops from the native vegetation using the MODIS NDVI satellite data. With that, the entire region was split into two land cover types, denoted here as desert and irrigation (that includes native vegetation along the river). Regional vegetation cover depends on both the desert and irrigated vegetation cover and their area fractions.

Regional vegetation cover in the downstream of the Heihe River Basin (2000–2012) was highly sensitive to variations in the area of irrigated land (Eq. 6). Over the whole

HESSD
11, 1529–1554, 2014

period we found that the contributions to regional vegetation cover change due to changes in irrigated vegetation cover (f_I) and the area fraction (A_I^*) were 7.8 and 20.5 % respectively, whilst changes in the non-irrigated vegetation cover (f_D) and area fraction (A_D^*) accounted for 75.8 and −4.1 %, respectively. This result implies that we need only consider variations in f_D and in A_I^* to account for most of the changes in regional vegetation cover.

In the desert regions we found that f_D was strongly related to annual precipitation as expected in such an arid region (Fig. 6). More importantly, we found that A_I^* in a given year was related to the runoff in the previous year. The underlying basis of that relation would be complex and would involve a lag because (i) farmers may anticipate future planting areas based on runoff from the previous year/s, and (ii) the runoff recharges the local groundwater that is subsequently used by the local population (for irrigation) and by the native oasis vegetation. The lagged relation between runoff and the area of irrigation may provide a useful empirical basis for forecasting and confirms the importance of managing the human impact to achieve targeted improvements in the regional ecology.

A number of studies have evaluated the ecological environment in Ejina since the Ecological Water Conveyance Project (EWCP) was launched in 2000. Some earlier work includes, for example, questionnaire surveys and group discussions (Wang et al., 2013), eco-hydrological field-based investigations (Guo et al., 2009; Wang et al., 2011; Zhang et al., 2011), monitoring by satellite remote sensing (Jin et al., 2010; Jia et al., 2011; Zhang et al., 2011) and by model simulation (Xi et al., 2010). Those studies revealed that more water is now available for the natural environment with plant growth extending up to 1000 m from the Heihe River (Guo et al., 2009). In addition the regional water table has risen in many parts of the Ejina Basin (Zhao et al., 2009; Wang et al., 2011). Native vegetation in most (~ 80 %) of the oasis regions has shown an increasing trend in the last decade (Zhang et al., 2011) in response to the increasing availability of water. Our results set these vegetation changes into a larger regional setting and we show that the changes have impacted on the regional vegetation cover.

HESSD
11, 1529–1554, 2014

The downstream parts of Heihe River basin studied here are typical of the oasis-desert landscape that dominates Central Asia with widespread irrigation. In this system, the allocation of water resources is critical in achieving a balance among different oases as well as between human water appropriation for irrigation and ecological conservation. A similar over use of water for irrigation also happened in the Aral Sea. The water withdrawal for irrigation led to a dramatic shrinkage of the Aral Sea that has attracted the attention of the international scientific community over the last few decades (Micklin, 1988; Whish-Wilson, 2002; Lioubimtseva et al., 2005). Rational distribution and sustainable management of water resources is still a long-term and arduous task. Our results suggest that it is possible to use remotely sensed data to provide practical support in assessing the ecological status of irrigation regions that surround most Central Asian rivers.

5 Conclusions

We found that the regional fractional vegetation cover f_V in the downstream parts of the greater Heihe River basin increased by 25 % from 2000 to 2012. The largest contribution was due to a slight greening of the desert regions that was consistent with increased precipitation over the period. The other main contribution to the regional trend was an expansion of irrigation (including native vegetation) along the Heihe River that was found to be dependent on the runoff in the previous year. In conclusion, water availability both from precipitation and runoff can explain around 52 % of the total variance in regional vegetation cover over the period in this extremely arid environment. This study showed that it is feasible to separate the variations in regional vegetation cover that are due to changes in the climate from those due to changes in human activities given appropriate regional context.

Supplementary material related to this article is available online at http://www.hydrol-earth-syst-sci-discuss.net/11/1529/2014/hessd-11-1529-2014-supplement.pdf.

HESSD
11, 1529–1554, 2014

Acknowledgements. This study was supported by the National Program on Key Basic Research Project of China (2010CB951003) and China Scholarship Council. Vegetation type data set is provided by Environmental and Ecological Science Data Center for West China, National Natural Science Foundation of China (http://westdc.westgis.ac.cn).

References

Angelini, I. M., Garstang, M., Davis, R. E., Hayden, B., Fitzjarrald, D. R., Legates, D. R., Greco, S., Macko, S., and Connors, V.: On the coupling between vegetation and the atmosphere, Theor. Appl. Climatol., 105, 243-261, doi:10.1007/s00704-010-0377-5, 2011.

Bonan, G. B., Levis, S., Sitch, S., Vertenstein, M., and Oleson, K. W.: A dynamic global vegetation model for use with climate models: concepts and description of simulated vegetation dynamics, Glob. Change Biol., 9, 1543–1566, doi:10.1046/j.1365-2486.2003.00681.x, 2003.

Bounoua, L., Hall, F. G., Sellers, P. J., Kumar, A., Collatz, G. J., Tucker, C. J., and Imhoff, M. L.: Quantifying the negative feedback of vegetation to greenhouse warming: a modeling approach, Geophys. Res. Lett., 37, L23701, doi:10.1029/2010gl045338, 2010.

Box, E. O., Holben, B. N., and Kalb, V.: Accuracy of the Avhrr vegetation index as a predictor of biomass, primary productivity and net CO_2 Flux, Vegetatio, 80, 71–89, doi:10.1007/Bf00048034, 1989.

Carlson, T. N. and Ripley, D. A.: On the relation between NDVI, fractional vegetation cover, and leaf area index, Remote Sens. Environ., 62, 241–252, doi:10.1016/S0034-4257(97)00104-1, 1997.

Chen, J., Jonsson, P., Tamura, M., Gu, Z. H., Matsushita, B., and Eklundh, L.: A simple method for reconstructing a high-quality NDVI time-series data set based on the Savitzky-Golay filter, Remote Sens. Environ., 91, 332–344, doi:10.1016/j.rse.2004.03.014, 2004.

Chen, M. Y., Xie, P. P., Janowiak, J. E., and Arkin, P. A.: Global land precipitation: a 50-yr monthly analysis based on gauge observations, J. Hydrometeorol., 3, 249–266, doi:10.1175/1525-7541(2002)003<0249:Glpaym>2.0.Co;2, 2002.

Donohue, R. J., McVicar, T. R., and Roderick, M. L.: Climate-related trends in Australian vegetation cover as inferred from satellite observations, 1981–2006, Glob. Change Biol., 15, 1025–1039, doi:10.1111/j.1365-2486.2008.01746.x, 2009.

HESSD
11, 1529–1554, 2014

Donohue, R. J., Roderick, M. L., McVicar, T. R., and Farquhar, G. D.: Impact of CO_2 fertilization on maximum foliage cover across the globe's warm, arid environments, Geophys. Res. Lett., 40, 3031–3035, doi:10.1002/grl.50563, 2013.

Fang, J. Y., Piao, S. L., He, J. S., and Ma, W. H.: Increasing terrestrial vegetation activity in China, 1982–1999, Science in China Series C: Life Sciences, 47, 229–240, doi:10.1007/BF03182768, 2004.

Fensholt, R., Rasmussen, K., Kaspersen, P., Huber, S., Horion, S., and Swinnen, E.: Assessing land degradation/recovery in the African Sahel from long-term earth observation based primary productivity and precipitation relationships, Remote Sens., 5, 664–686, doi:10.3390/Rs5020664, 2013.

Fu, K., Chen, X. P., Liu, Q. G., and Li, C. H.: Land use and land cover changes based on remote sensing and GIS in Heihe River basin, in: IEEE International Geoscience and Remote Sensing Symposium, Barcelona, Spain, 23–28 July, 1790–1793, 2007.

GeoHive, available at: http://www.geohive.com/cntry/cn-15.aspx, last access: 1 May 2013, 2010.

Gerten, D., Schaphoff, S., Haberlandt, U., Lucht, W., and Sitch, S.: Terrestrial vegetation and water balance – hydrological evaluation of a dynamic global vegetation model, J. Hydrol., 286, 249–270, doi:10.1016/j.jhydrol.2003.09.029, 2004.

Guo, Q. L., Feng, Q., and Li, J. L.: Environmental changes after ecological water conveyance in the lower reaches of Heihe River, northwest China, Environ. Geol., 58, 1387–1396, doi:10.1007/s00254-008-1641-1, 2009.

Harris, I., Jones, P., Osborn, T., and Lister, D.: Updated high-resolution grids of monthly climatic observations–the CRU TS3.10 Dataset, Int. J. Climatol., in press, 2014.

Herrmann, S. M., Anyamba, A., and Tucker, C. J.: Recent trends in vegetation dynamics in the African Sahel and their relationship to climate, Global Environ. Chang., 15, 394–404, doi:10.1016/j.gloenvcha.2005.08.004, 2005.

Jia, L., Shang, H., Hu, G., and Menenti, M.: Phenological response of vegetation to upstream river flow in the Heihe Rive basin by time series analysis of MODIS data, Hydrol. Earth Syst. Sci., 15, 1047–1064, doi:10.5194/hess-15-1047-2011, 2011.

Jin, X. M., Schaepman, M., Clevers, J., Su, Z. B., and Hu, G. C.: Correlation between annual runoff in the Heihe River to the vegetation cover in the Ejina Oasis (China), Arid Land. Res. Manag., 24, 31–41, doi:10.1080/15324980903439297, 2010.

HESSD
11, 1529–1554, 2014

Lioubimtseva, E., Cole, R., Adams, J. M., and Kapustin, G.: Impacts of climate and land-cover changes in arid lands of Central Asia, J Arid Environ, 62, 285–308, doi:10.1016/j.jaridenv.2004.11.005, 2005.

Lioubimtseva, E. and Henebry, G. M.: Climate and environmental change in arid Central Asia: impacts, vulnerability, and adaptations, J. Arid. Environ., 73, 963–977, doi:10.1016/j.jaridenv.2009.04.022, 2009.

Micklin, P. P.: Desiccation of the Aral Sea – a water management disaster in the Soviet-Union, Science, 241, 1170–1175, doi:10.1126/science.241.4870.1170, 1988.

Mohammat, A., Wang, X. H., Xu, X. T., Peng, L. Q., Yang, Y., Zhang, X. P., Myneni, R. B., and Piao, S. L.: Drought and spring cooling induced recent decrease in vegetation growth in Inner Asia, Agr. Forest Meteorol., 178, 21–30, doi:10.1016/j.agrformet.2012.09.014, 2013.

Myneni, R. B., Keeling, C. D., Tucker, C. J., Asrar, G., and Nemani, R. R.: Increased plant growth in the northern high latitudes from 1981 to 1991, Nature, 386, 698–702, doi:10.1038/386698a0, 1997.

NASA: National Aeronautics and Space Administration Earth Observing System Data and Information System, available at: http://reverb.echo.nasa.gov/, last access: 13 March 2013.

Nemani, R. R., Keeling, C. D., Hashimoto, H., Jolly, W. M., Piper, S. C., Tucker, C. J., Myneni, R. B., and Running, S. W.: Climate-driven increases in global terrestrial net primary production from 1982 to 1999, Science, 300, 1560–1563, doi:10.1126/science.1082750, 2003.

Pielke, R. A., Avissar, R., Raupach, M., Dolman, A. J., Zeng, X. B., and Denning, A. S.: Interactions between the atmosphere and terrestrial ecosystems: influence on weather and climate, Glob. Change Biol., 4, 461–475, doi:10.1046/j.1365-2486.1998.t01-1-00176.x, 1998.

Qin, D. J., Zhao, Z. F., Han, L. F., Qian, Y. P., Ou, L., Wu, Z. Q., and Wang, M. C.: Determination of groundwater recharge regime and flowpath in the Lower Heihe River basin in an arid area of Northwest China by using environmental tracers: implications for vegetation degradation in the Ejina Oasis, Appl. Geochem., 27, 1133–1145, doi:10.1016/j.apgeochem.2012.02.031, 2012.

Rahimov, S.: Impacts of climate change on water resources in Central Asia, CIDOB Asia Documents, Barcelona Centre for International Affairs (CIDOB), Barcelona, Spain, 25, 33–55, 2009.

HESSD
11, 1529–1554, 2014

Schneider, U., Fuchs, T., Meyer-Christoffer, A., and Rudolf, B.: Global precipitation analysis products of the GPCC, Global Precipitation Climatology Centre (GPCC), DWD, Internet Publikation, available at: http://gpcc.dwd.de, last access: 20 March 2013, 1–12, 2008.

Sun, F. B., Roderick, M. L., and Farquhar, G. D.: Changes in the variability of global land precipitation, Geophys. Res. Lett., 39, L19402, doi:10.1029/2012gl053369, 2012.

Tucker, C. J.: Red and photographic infrared linear combinations for monitoring vegetation, Remote Sens. Environ., 8, 127–150, doi:10.1016/0034-4257(79)90013-0, 1979.

Unger-Shayesteh, K., Vorogushyn, S., Farinotti, D., Gafurov, A., Duethmann, D., Mandychev, A., and Merz, B.: What do we know about past changes in the water cycle of Central Asian headwaters? A review, Global Planet. Change, 110, 4–25, doi:10.1016/j.gloplacha.2013.02.004, 2013.

Wang, P., Zhang, Y. C., Yu, J. J., Fu, G. B., and Ao, F.: Vegetation dynamics induced by groundwater fluctuations in the lower Heihe River Basin, northwestern China, J. Plant. Ecol.-UK, 4, 77–90, doi:10.1093/Jpe/Rtr002, 2011.

Wang, Y., Feng, Q., Chen, L. J., and Yu, T. F.: Significance and effect of ecological rehabilitation project in inland river basins in Northwest China, Environ. Manage., 52, 209–220, doi:10.1007/s00267-013-0077-x, 2013.

Whish-Wilson, P.: The Aral Sea environmental health crisis, Journal of Rural and Remote Environmental Health, 1, 29–34, 2002.

Xi, H. Y., Feng, Q., Liu, W., Si, J. H., Chang, Z. Q., and Su, Y. H.: The research of groundwater flow model in Ejina Basin, Northwestern China, Environmental Earth Sciences, 60, 953–963, doi:10.1007/s12665-009-0231-1, 2010.

Yao, T. D., Wang, Y. Q., Liu, S. Y., Pu, J. C., Shen, Y. P., and Lu, A. X.: Recent glacial retreat in High Asia in China and its impact on water resource in Northwest China, Science in China Series D: Earth Sciences, 47, 1065–1075, doi:10.1360/03yd0256, 2004.

Zhang, Y. C., Yu, J. J., Wang, P., and Fu, G. B.: Vegetation responses to integrated water management in the Ejina basin, northwest China, Hydrol. Process., 25, 3448–3461, doi:10.1002/Hyp.8073, 2011.

Zhao, C., Li, S., Feng, Z., and Shen, W.: Dynamics of groundwater level in the water table fluctuant belt at the lower reaches of Heihe River, Journal of Desert Research, 29, 365–370, 2009.

HESSD
11, 1529–1554, 2014

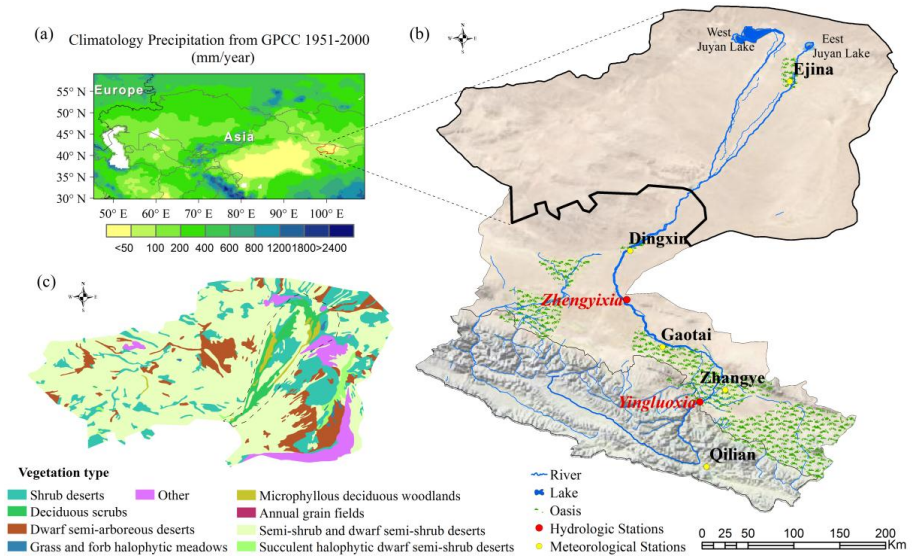

Fig. 1. Details of the study area. **(a)** Regional setting and the mean annual precipitation (1951–2000). **(b)** Landscape of Heihe River Basin with location of meteorological and hydrologic observation sites. **(c)** Vegetation Map of lower Heihe river basin where the dashed line denotes the bounds of the possible irrigation area.

HESSD
11, 1529–1554, 2014

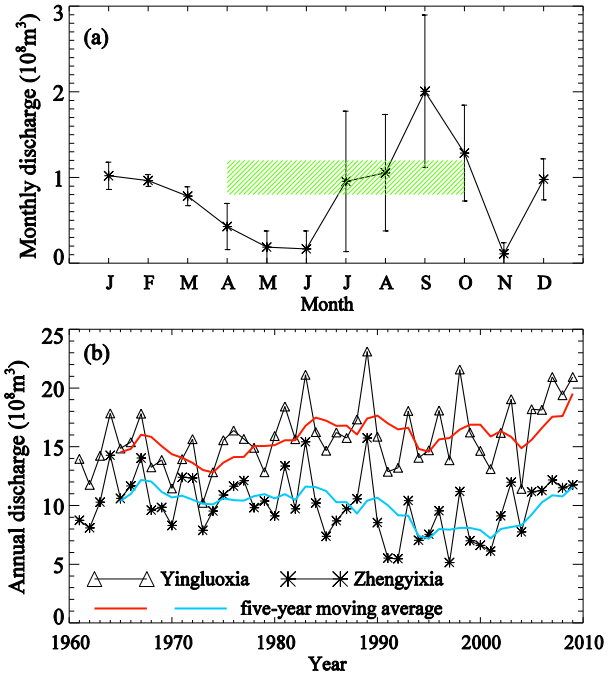

Fig. 2. River flows in the Heihe River basin. **(a)** Mean monthly river discharge (bars indicate standard deviation) of Heihe River (2000–2009) at Zhengyixia station in relation to the growing season (diagonal stripes). **(b)** Annual discharge of Heihe River (1961–2009) at Yingluoxia and Zhengyixia stations

HESSD
11, 1529–1554, 2014

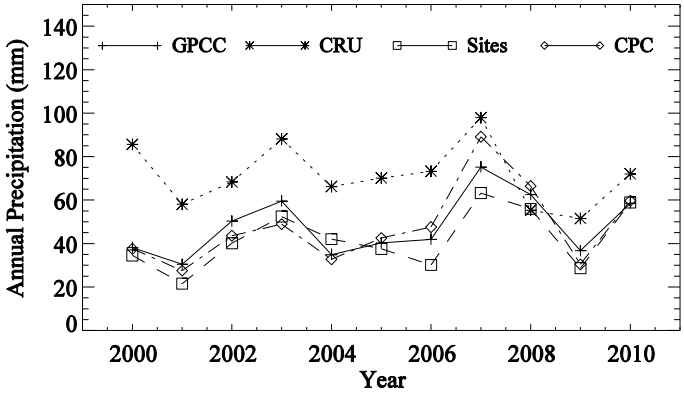

Fig. 3. Annual precipitation for the study area as per four different data sources (as indicated).

HESSD
11, 1529–1554, 2014

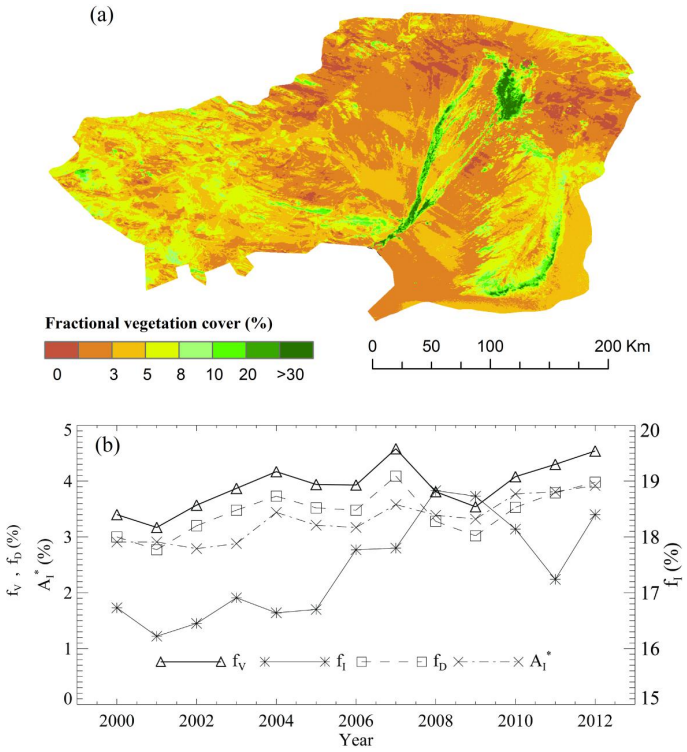

Fig. 4. Vegetation cover and trends. **(a)** Growing season (April–October) mean annual fractional vegetation cover (2000–2012). **(b)** Trends in the growing season (April–October) mean annual fractional vegetation for the whole region (f_V, left scale), desert (f_D, 3 left scale) and irrigated (f_I, right scale) land cover classes, and for the fractional area of irrigation (A_I^*, left scale).

HESSD
11, 1529–1554, 2014

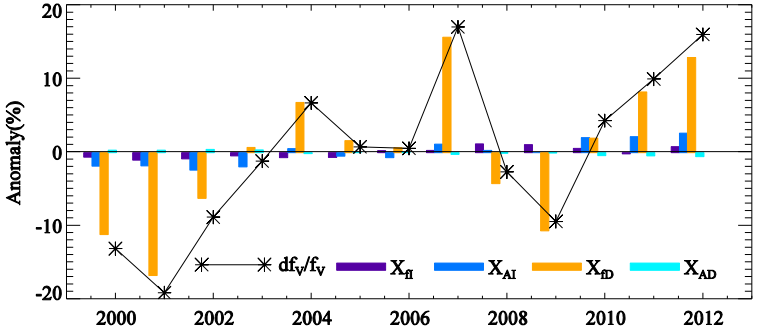

Fig. 5. Annual changes in relative vegetation cover (df_V/f_V) and the underlying components from mean annual fractional vegetation for the desert (X_{fD}), for the irrigated (X_{fI}), and for the fractional area of irrigation (X_{AI},) and desert (X_{AD}).

HESSD
11, 1529–1554, 2014

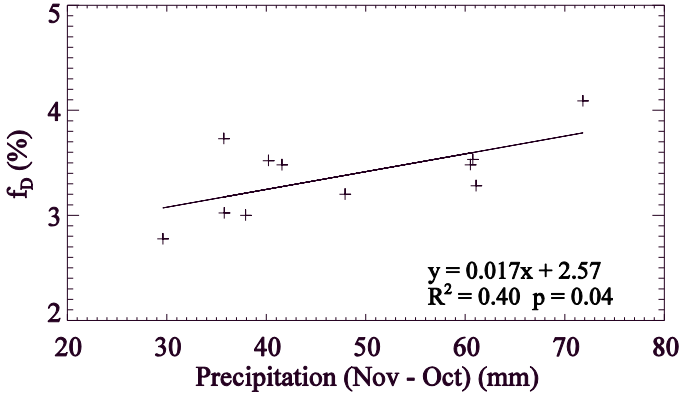

Fig. 6. Relationship between growing season desert vegetation cover (f_D) and precipitation (per GPCC database).

HESSD
11, 1529–1554, 2014

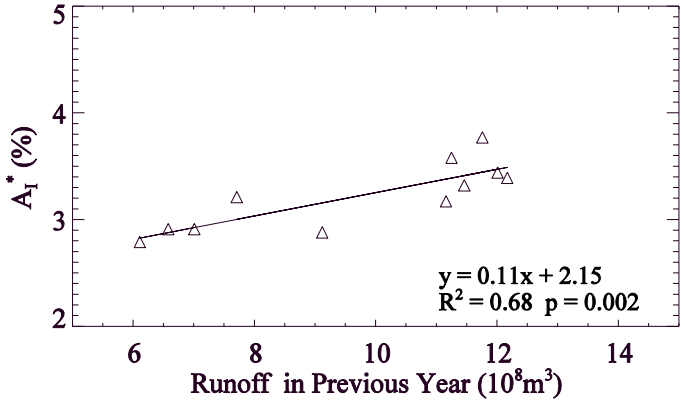

Fig. 7. Relationship between fractional irrigated area A_I^* and runoff at Zhengyixia from the previous year.

HESSD
11, 1529–1554, 2014

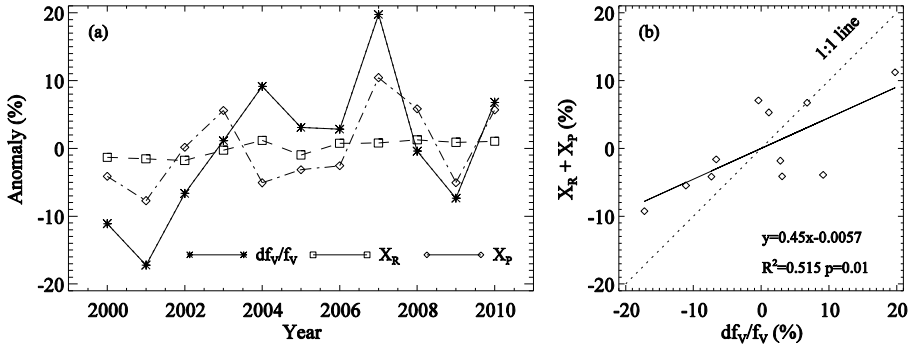

Fig. 8. Relation between regional vegetaion cover and water availability. **(a)** Relative variations, and **(b)** the observed annual changes in relative vegetation cover (df_V/f_V) vs. predicted changes from water availability of runoff (X_R) and precipitation (X_P).

HESSD
11, 1529–1554, 2014